

# Transcriptomics of a THEV-infected Turkey B-cell Line

Abraham Quaye<sup>†,a</sup>, Brian D. Poole<sup>a,\*</sup>

<sup>a</sup>Department of Microbiology and Molecular Biology, Brigham Young University

<sup>†</sup>First-author

<sup>\*</sup>Corresponding Author

## Corresponding Author Information

brian\_poole@byu.edu

Department of Microbiology and Molecular Biology,

4007 Life Sciences Building (LSB),

Brigham Young University,

Provo, Utah

<sup>14</sup> **ABSTRACT**

## 15 INTRODUCTION

16 Turkey hemorrhagic enteritis virus (THEV), belonging to the family *Adenoviridae*, genus *Siadenovirus*,  
17 infects turkeys, chickens, and pheasants (1, 2). Infecting its hosts via the feco-oral route, THEV causes  
18 hemorrhagic enteritis (HE) in turkeys, a debilitating disease affecting predominantly 6-12 week old turkey  
19 poults characterized by immunosuppression (IMS), depression, splenomegaly, intestinal lesions leading to  
20 bloody droppings, and up to 80% mortality (3–6). The clinical disease usually persists in affected flocks for  
21 about 7-10 days. However, secondary bacterial infections may extend the duration of illness and mortality for  
22 an additional 2-3 weeks due to the immunosuppressive nature of the virus, exacerbating the economic losses  
23 (5, 7). Low pathogenic (avirulent) strains of THEV have been isolated, which show subclinical infections  
24 but retain the immunosuppressive effects. Since its isolation from a pheasant spleen, the Virginia Avirulent  
25 Strain (VAS) has been used effectively as a live vaccine despite the immunosuppressive side-effects but  
26 the vaccinated birds are rendered more susceptible to opportunistic infections and death than unvaccinated  
27 cohorts leading to significant economic losses (4, 5, 8–10).

28 It is well-established that THEV primarily infects and replicates in turkey B-cells of the bursa and spleen and  
29 somewhat in macrophages, inducing apoptosis and necrosis. Consequently, a significant drop in number of  
30 B-cells (specifically, IgM+ B-cells) and macrophages ensue along with increased T-cell counts with abnormal  
31 T-cell subpopulation (CD4+ and CD8+) ratios. The cell death seen in the B-cells and macrophages is  
32 generally proposed as the major cause of THEV-induced IMS as both humoral and cell-mediated immunity  
33 are impaired (5, 6, 8, 11). It is also thought that the virus replication in the spleen attracts T-cells and  
34 peripheral blood macrophages to the spleen where the T-cells are activated by cytokines from activated  
35 macrophages and vice versa. The activated T-cells undergo clonal expansion and secrete interferons: type I  
36 (IFN- $\alpha$  and IFN- $\beta$ ) and type II (IFN- $\gamma$ ) as well as tumor necrosis factor (TNF) while activated macrophages  
37 secrete interleukin 6 (IL-6), TNF, and nitric oxide (NO), an antiviral agent with immunosuppressive properties.  
38 The inflammatory cytokines released by T-cells and macrophages (e.g., TNF and IL-6) may also induce  
39 apoptosis in bystander splenocytes, exacerbating the already numerous apoptotic and necrotic splenocytes,  
40 culminating in IMS (8, 11) (see **Figure 1**). However, the precise molecular mechanisms of THEV-induced  
41 IMS or pathways involved are poorly understood (6). Elucidating the specific mechanisms and pathways of  
42 THEV-induced IMS is the most crucial step in THEV research as it will present a means of mitigating the IMS.

43 Next generation sequencing (NGS) is a groundbreaking technology that has significantly enhanced our  
44 understanding of DNA and RNA structure and function, and facilitated exceptional advancements in all  
45 domains of biology and the Life Sciences, including rare genetic diseases, cancer genomics, microbiome  
46 analysis, infectious diseases, and population genetics (12). mRNA sequencing (RNA-seq), an NGS approach

to transcriptomic studies, is a versatile, high throughput, and cost-effective technology that allows a broad scan of the entire transcriptome (the complete set of RNA molecules produced under specific conditions or in specific cells), thereby uncovering the active molecular pathways and processes. This technology has been leveraged in uncountable number of studies to elucidate cellular mechanisms under a wide range of treatment conditions, including virus-infected versus uninfected transcriptome comparisons (12–16). In RNA-seq studies, differentially expressed genes (DEGs) identified under different experimental conditions are key to unlocking the interesting biology or mechanism under study.

To the best of our knowledge, no studies have been done leveraging the wealth of information offered by RNA-seq to elucidate the molecular mechanisms and pathways leading to THEV-induced IMS. To effectively counteract the immunosuppressive effect of the vaccine, it is essential to unravel the host mechanisms/pathways influenced by the virus to bring about IMS. In this work, we present the first transcriptome profile analysis of THEV-infected turkey MDTC-RP19 B-cells by paired-end RNA-seq, highlighting specific host cellular/molecular processes affected during a THEV infection. Our paired-end sequencing allowed for reading 149 bp long high quality (mean Phred Score of 36) sequences from each end of cDNA fragments, which were mapped to the genome of domestic turkey (*Meleagris gallopavo*). \*\*\*put overview of results here





## 64 CONCLUSIONS

## MATERIALS AND METHODS

### Cell culture and THEV Infection

The Turkey B-cell line (MDTC-RP19, ATCC CRL-8135) was grown as suspension cultures in 1:1 complete Leibovitz's L-15/McCoy's 5A medium with 10% fetal bovine serum (FBS), 20% chicken serum (ChS), 5% tryptose phosphate broth (TPB), and 1% antibiotic solution (100 U/mL Penicillin and 100 µg/mL Streptomycin), at 41°C in a humidified atmosphere with 5% CO<sub>2</sub>. Infected cells were maintained in 1:1 serum-reduced Leibovitz's L15/McCoy's 5A media (SRLM) with 2.5% FBS, 5% ChS, 1.2% TPB, and 1% antibiotic solution. A commercially available THEV vaccine was purchased from Hygieia Biological Labs (VAS strain). The stock virus was titrated using an in-house qPCR assay with titer expressed as genome copy number (GCN)/mL, similar to Mahshoub *et al* (17) with modifications. Cells were infected in triplicate at a multiplicity of infection (MOI) of 100 GCN/cell, incubated at 41°C for 1 hour, and washed three times with phosphate buffered saline (PBS) to get rid of free virus particles. Triplicate samples were harvested at 4-, 12-, 24-, and 72-hpi for total RNA extraction.

### RNA extraction and Sequencing

Total RNA was extracted from infected cells using the ThermoFisher RNAqueous™-4PCR Total RNA Isolation Kit (which includes a DNase I digestion step) per manufacturer's instructions. An agarose gel electrophoresis was performed to check RNA integrity. The RNA quantity and purity was initially assessed using nanodrop, and RNA was used only if the A260/A280 ratio was  $2.0 \pm 0.05$  and the A260/A230 ratio was  $>2$  and  $<2.2$ . Extracted total RNA samples were sent to LC Sciences, Houston TX for poly-A-tailed mRNA sequencing where RNA integrity was checked with Agilent Technologies 2100 Bioanalyzer High Sensitivity DNA Chip and poly(A) RNA-seq library was prepared following Illumina's TruSeq-stranded-mRNA sample preparation protocol. Paired-end sequencing, generating 150 bp reads was performed on the Illumina NovaSeq 6000 sequencing system. The paired-end 150bp sequences obtained during this study and all expression data have been submitted to the Gene Expression Omnibus database, under accession no #####

### Quality Control and Mapping Process

Sequencing reads were processed following a well-established protocol described by Pertea *et al* (18), using Snakemake - version 7.32.4 (19), a popular workflow management system to drive the pipeline. Briefly, raw sequencing reads were trimmed with Cutadapt - version 1.10 (20) and the quality of trimmed reads evaluated using the FastQC software, version 0.12.1 (Bioinformatics Group at the Babraham Institute, Cambridge, United Kingdom; [www.bioinformatics.babraham.ac.uk](http://www.bioinformatics.babraham.ac.uk)), achieving an overall Mean Sequence Quality (Phred Score) of 36. Trimmed reads were mapped the reference *Meleagris gallopavo* genome ([https://ftp.ncbi.nlm.nih.gov/genomes/all/GCF/000/146/605/GCF\\_000146605.3\\_Turkey\\_5.1/GCF\\_000146](https://ftp.ncbi.nlm.nih.gov/genomes/all/GCF/000/146/605/GCF_000146605.3_Turkey_5.1/GCF_000146)



97 605.3\_Turkey\_5.1\_genomic.fna.gz) with Hisat2 - version 2.2.1 (18) using the accompanying gene transfer  
98 format (GTF) annotation file ([https://ftp.ncbi.nlm.nih.gov/genomes/all/GCF/000/146/605/GCF\\_000146605.3](https://ftp.ncbi.nlm.nih.gov/genomes/all/GCF/000/146/605/GCF_000146605.3)  
99 \_Turkey\_5.1/GCF\_000146605.3\_Turkey\_5.1\_genomic.gtf.gz) to build a genomic index. Samtools - version  
100 1.19.2 was used to convert the output Sequence Alignment Map (SAM) file to the more manageable Binary  
101 Alignment Map (BAM) format. The StringTie (v2.2.1) software (18), set to expression estimation mode was  
102 used to generate normalized gene expression estimates from the BAM files for genes in the reference GTF  
103 file after which the prepDE.py3 script was used to extract read count information from the StringTie gene  
104 expression files, providing an expression-count matrix for downstream DEG analysis.

#### 105 **DEG Analysis and Functional Enrichment Analysis**

106 DEG analysis between mock- and THEV-infected samples was performed using very popular DESeq2 (21),  
107 which employs a Negative Binomial distribution model for read count comparisons. Genes with  $P_{\text{adjusted}}$ -value  
108  $\leq 0.05$  were considered as differentially expressed. The data is deposited at GEO under accession number  
109 ###

#### 110 **Expression Profiling and Differentially Expressed Genes**

#### 111 **Quantitative Real-Time Reverse Transcriptase PCR**

#### 112 **Statistical Analysis**







## 116 REFERENCES

- 117 1. Harrach B. 2008. Adenoviruses: General features, p. 1–9. *In* Mahy, BWJ, Van Regenmortel, MHV (eds.), Encyclopedia of virology (third edition). Book Section. Academic Press, Oxford.
- 118 2. Davison A, Benko M, Harrach B. 2003. Genetic content and evolution of adenoviruses. The Journal of general virology 84:2895–908.
- 119 3. Gross WB, Moore WE. 1967. Hemorrhagic enteritis of turkeys. Avian Dis 11:296–307.
- 120 4. Beach NM. 2006. Characterization of avirulent turkey hemorrhagic enteritis virus: A study of the molecular basis for variation in virulence and the occurrence of persistent infection. Thesis.
- 121 5. Dhama K, Gowthaman V, Karthik K, Tiwari R, Sachan S, Kumar MA, Palanivelu M, Malik YS, Singh RK, Munir M. 2017. Haemorrhagic enteritis of turkeys – current knowledge. Veterinary Quarterly 37:31–42.
- 122 6. Tykałowski B, Śmiałek M, Koncicki A, Ognik K, Zduńczyk Z, Jankowski J. 2019. The immune response of young turkeys to haemorrhagic enteritis virus infection at different levels and sources of methionine in the diet. BMC Veterinary Research 15.
- 123 7. Pierson F, Fitzgerald S. 2008. Hemorrhagic enteritis and related infections. Diseases of Poultry 276–286.
- 124 8. Rautenschlein S, Sharma JM. 2000. Immunopathogenesis of haemorrhagic enteritis virus (HEV) in turkeys. Dev Comp Immunol 24:237–46.
- 125 9. Larsen CT, Domermuth CH, Sponenberg DP, Gross WB. 1985. Colibacillosis of turkeys exacerbated by hemorrhagic enteritis virus. Laboratory studies. Avian Dis 29:729–32.

- 126 10. Beach NM, Duncan RB, Larsen CT, Meng XJ, Sriranganathan N, Pierson FW. 2009. Persistent infection of turkeys with an avirulent strain of turkey hemorrhagic enteritis virus. *Avian Diseases* 53:370–375.
- 127 11. Rautenschlein S, Suresh M, Sharma JM. 2000. Pathogenic avian adenovirus type II induces apoptosis in turkey spleen cells. *Archives of Virology* 145:1671–1683.
- 128 12. Satam H, Joshi K, Mangrolia U, Waghoo S, Zaidi G, Rawool S, Thakare RP, Banday S, Mishra AK, Das G, Malonia SK. 2023. Next-generation sequencing technology: Current trends and advancements. *Biology* 12:997.
- 129 13. Pandey D, Onkara Perumal P. 2023. A scoping review on deep learning for next-generation RNA-seq. Data analysis. *Functional & Integrative Genomics* 23.
- 130 14. Wang B, Kumar V, Olson A, Ware D. 2019. Reviving the transcriptome studies: An insight into the emergence of single-molecule transcriptome sequencing. *Frontiers in Genetics* 10.
- 131 15. Choi SC. 2016. On the study of microbial transcriptomes using second- and third-generation sequencing technologies. *Journal of Microbiology* 54:527–536.
- 132 16. Mo Q, Feng K, Dai S, Wu Q, Zhang Z, Ali A, Deng F, Wang H, Ning Y-J. 2023. Transcriptome profiling highlights regulated biological processes and type III interferon antiviral responses upon crimean-congo hemorrhagic fever virus infection. *Virologica Sinica* 38:34–46.
- 133 17. Mahsoub HM, Evans NP, Beach NM, Yuan L, Zimmerman K, Pierson FW. 2017. Real-time PCR-based infectivity assay for the titration of turkey hemorrhagic enteritis virus, an adenovirus, in live vaccines. *Journal of Virological Methods* 239:42–49.
- 134 18. Pertea M, Kim D, Pertea GM, Leek JT, Salzberg SL. 2016. Transcript-level expression analysis of RNA-seq experiments with HISAT, StringTie and ballgown. *Nature Protocols* 11:1650–1667.

- <sup>135</sup> 19. Mölder F, Jablonski KP, Letcher B, Hall MB, Tomkins-Tinch CH, Sochat V, Forster J, Lee S, Twardziok SO, Kanitz A, Wilm A, Holtgrewe M, Rahmann S, Nahnsen S, Köster J. 2021. Sustainable data analysis with snakemake. *F1000Research* 10:33.
- <sup>136</sup> 20. Martin M. 2011. Cutadapt removes adapter sequences from high-throughput sequencing reads. *EMBnetjournal* 17:10.
- <sup>137</sup> 21. Love MI, Huber W, Anders S. 2014. Moderated estimation of fold change and dispersion for RNA-seq data with DESeq2. *Genome Biology* 15:550.

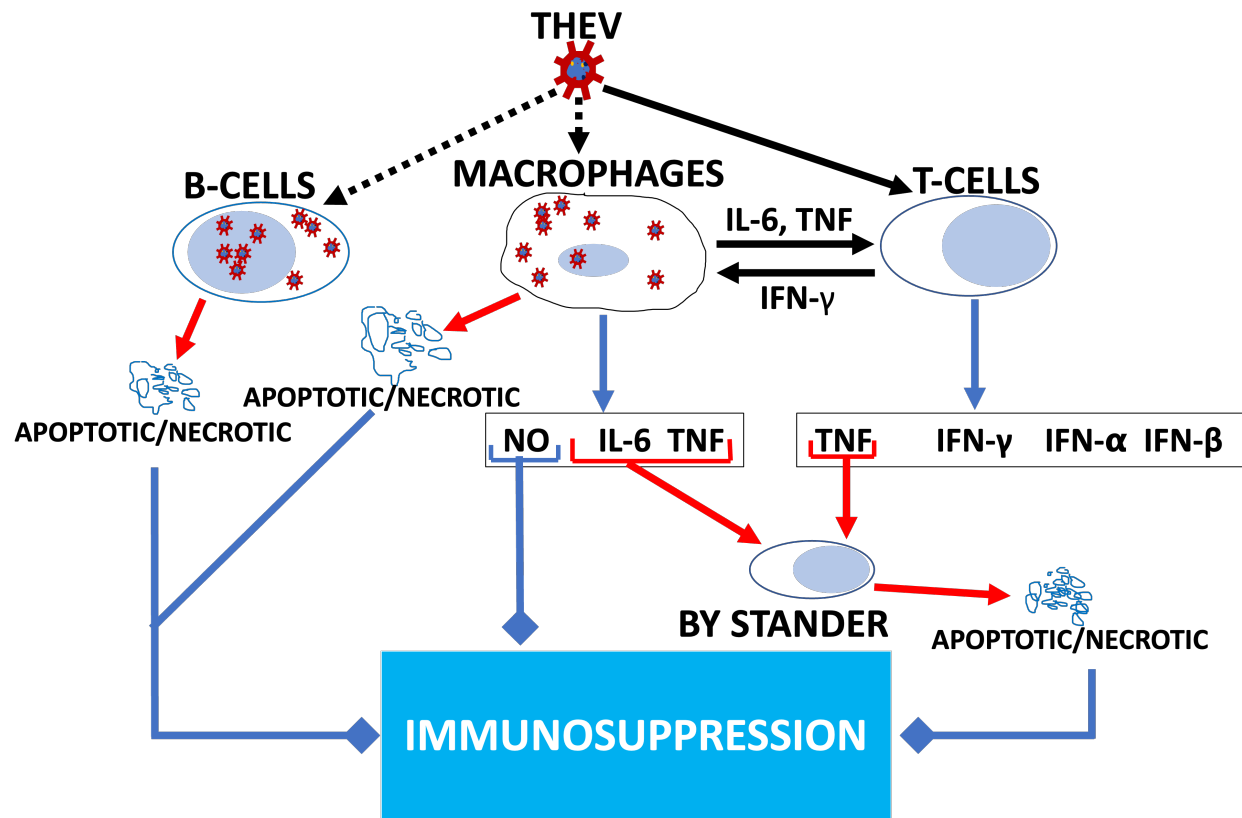


**Figure 1: Model of THEV-induced immunosuppression in turkeys.** THEV infection of target cells is indicated with black dotted arrows. Black unbroken arrows indicate cell activation. Red arrows indicated signals leading to apoptosis. Blue arrows indicate all cytokines released by the cell. Blue arrows with square heads indicated an event leading to IMS. Adapted from ((8))



Table 1: Summary of sequencing, quality control, and mapping processes

Sample	Raw Reads <sup>M</sup>	Trimmed Reads <sup>M</sup>	Mapped Reads <sup>M</sup>	Uniquely Mapped Reads <sup>M</sup>	Non-uniquely Mapped Reads <sup>M</sup>	Q20%	Q30%	GC Content (%)
I_12hrsS1 <sup>Inf</sup>	40.6	39.0	34.7 (88.92%)	33.1 (84.78%)	1.6 (4.14%)	99.95	97.23	47.5
I_12hrsS3 <sup>Inf</sup>	38.8	37.3	33.1 (88.78%)	31.7 (84.95%)	1.4 (3.83%)	99.95	97.53	47.5
I_24hrsS1 <sup>Inf</sup>	42.7	41.0	36.2 (88.13%)	34.5 (84.2%)	1.6 (3.93%)	99.95	96.95	46.5
I_24hrsS2 <sup>Inf</sup>	42.0	40.4	35.6 (88.1%)	33.9 (83.83%)	1.7 (4.27%)	99.94	97.05	46.5
I_24hrsS3 <sup>Inf</sup>	40.5	38.9	34.2 (88.01%)	32.7 (84.12%)	1.5 (3.89%)	99.95	97.08	47.0
I_4hrsS1 <sup>Inf</sup>	39.1	37.4	33 (88.16%)	31.2 (83.43%)	1.8 (4.73%)	99.93	97.04	48.5
I_4hrsS2 <sup>Inf</sup>	41.3	39.6	35.3 (89.24%)	33.6 (84.92%)	1.7 (4.33%)	99.95	97.15	47.0
I_4hrsS3 <sup>Inf</sup>	41.5	39.8	35.5 (89.2%)	33.2 (83.29%)	2.4 (5.91%)	99.95	97.11	47.5
I_72hrsS1 <sup>Inf</sup>	41.2	39.8	28.3 (71.09%)	26.9 (67.7%)	1.3 (3.38%)	99.96	97.23	44.5
I_72hrsS2 <sup>Inf</sup>	39.3	38.0	27 (71.11%)	25.8 (67.86%)	1.2 (3.25%)	99.96	97.34	44.5
I_72hrsS3 <sup>Inf</sup>	39.9	37.1	28.3 (76.36%)	26.1 (70.3%)	2.2 (6.05%)	99.87	96.14	52.5
U_12hrsN1 <sup>Mk</sup>	42.1	40.4	35.9 (88.72%)	34.1 (84.39%)	1.7 (4.33%)	99.95	97.04	47.5
U_12hrsN2 <sup>Mk</sup>	41.0	39.3	34.7 (88.4%)	33.2 (84.53%)	1.5 (3.86%)	99.94	97.08	47.5
U_24hrsN1 <sup>Mk</sup>	38.4	37.0	32.7 (88.46%)	31.4 (84.74%)	1.4 (3.72%)	99.96	97.48	47.5
U_24hrsN2 <sup>Mk</sup>	39.9	38.4	34 (88.58%)	32.6 (84.96%)	1.4 (3.61%)	99.95	96.95	47.0
U_4hrsN1 <sup>Mk</sup>	39.4	37.9	33.7 (88.9%)	32 (84.41%)	1.7 (4.49%)	99.96	97.36	47.0
U_4hrsN2 <sup>Mk</sup>	37.6	34.7	22 (63.43%)	18.5 (53.18%)	3.6 (10.25%)	99.80	94.96	61.0
U_72hrsN1 <sup>Mk</sup>	50.3	47.9	15.5 (32.4%)	11.7 (24.5%)	3.8 (7.9%)	99.88	96.54	56.0

Sample	Raw Reads <sup>M</sup>	Trimmed Reads <sup>M</sup>	Mapped Reads <sup>M</sup>	Uniquely Mapped Reads <sup>M</sup>	Non-uniquely Mapped Reads <sup>M</sup>	Q20%	Q30%	GC Content (%)
U_72hrsN2 <sup>Mk</sup>	40.5	38.9	34.5 (88.82%)	32.7 (84.14%)	1.8 (4.68%)	99.95	97.04	46.5

<sup>M</sup>All values for number of reads are in millions;

<sup>Inf</sup>These are infected samples indicated by the letter 'I' and 'S' in sample names

<sup>Mk</sup>These are mock-infected samples indicated by the letters 'U' and 'N' in sample names

